Chapter 11

Laser-Based Fabrication for Microfluidics Devices on Glass for Medical Applications

Daniel Nieto García and Gerard O'Connor

Additional information is available at the end of the chapter

http://dx.doi.org/10.5772/64324

Abstract

We report a laser-based process for microstructuring glass materials for microfluidics applications. The hybrid technique is composed of a nanosecond Q-Switch Nd:YVO_4 laser for fabricating the initial microfluidic microstructures on soda-lime glass substrates and a thermal treatment for reshaping and improving its morphological and optical qualities. The proposed technique preserves the advantages of the laser direct-write technique in terms of design flexibility, simplicity, fast prototyping, low cost, and so on. The beam spot size, pulse overlapping, ablation threshold, debris deposition, heating temperature, and time are investigated and optimized for fabricating optimal microfluidics structures on glass. The manufactured chips for circulating tumor cells (CTCs) capture were tested with tumor cells (Hec 1A) after being functionalized with an EpCAM antibody coating. Cells were successfully arrested on the pillars after being flown through the device giving our technology a translational application in the field of cancer research.

Keywords: Laser microstructuring, microchannels, glass, microfluidics devices

1. Introduction

Microfluidics is a fast developing engineering science that controls the flow of minute amounts of liquids or gases in a miniaturized system in an increasing number of applications such as biomedical diagnostic, microfuel cells, and cooling in microelectronics [1–4]. The microfluidic devices are used in making rapid inroads in the modern analytical laboratory primarily because of their small physical footprint, speed and efficiency of chemical separations, and reduced reagent consumption. These applications demand transparent materials that permit high-resolution imaging, fluorescence microscopy, and also to analyze parameters such as laminar flow, mass transport driven by diffusion rather than turbulence, and constant removal of waste products [5–7].

Traditionally, lab-on-a-chip devices have been manufactured by silica due to its well-understood surface chemistry and favorable micromachining techniques that are ubiquitous in the microelectronics industry. Recently, researchers have begun to utilize devices fabricated from polymer substrates as an alternative to glass, although glass may still be the preferred materials in clinical medicine, biology, and chemistry. Microchannels fabricated on glass have a growing importance in the miniaturization of microfluidic devices for chemical and biological micro-total analysis system.

Glass materials are commonly used due to the beneficial optical properties, surface stability, and solvent compatibility, as well as due to the straightforward and well-understood fabrication techniques [8–10]. The mechanical rigidity, chemical resistance, and low-permeability properties of glass, combined with their optical transparency, make it a good choice for many demanding lab-on-a-chip applications. Glass materials overcome some limitations of polymers, they are reusable and have low autofluorescence and smooth surfaces. Nevertheless, the high cost of processing glass and of the material itself limit the use of glass as disposable devices. Two different approaches challenging demands to be solved on microfluidics, high-quality devices made of glass and disposable low-cost devices made of plastic.

There are large and well-developed micromachining methods for fabricating microfluidic devices on glass, the choice among them depends on the materials to be treated, and the size and shape of the required features. Embossing, injection molding, and other thermoforming techniques provide high throughput and cost, but are ineffective for glass [11]. Because lithography techniques require advanced facilities and numerous process steps, numerous researchers have explored the fabrication of channels in glass using other technologies, such as electron beam lithography, photolithography, and dry and wet etching [12–15].

Some of these techniques provide high-quality microfluidic systems, but require sophisticated equipment located in clean rooms and with the inconvenient of production toxic waste, which in terms of microfabrication means that there are significant challenges in fabricating low-cost and reliable microchannels in glass. For example, the surface roughness in a microchannel can be caused by an inaccurate and imprecise alignment of the mask used in the fabrication process.

Laser has become increasingly important in recent years for many fields, including microoptics, microelectronics, microbiology, and microchemistry. High micromachining quality with ns-pulse and fs-pulse lasers was demonstrated for direct ablation of dielectrics. Laser micromachining offers a single-step method for direct writing of microchannels in glass. Using this laser ablation technique, it is possible to fabricate geometries with variable depth and high aspect ratio that cannot be achieved through traditional microlithographic techniques. Laser ablation, because of its noncontact nature, allows the micromachining and surface patterning of glass materials with minimal mechanical and thermal deformation. Due to the low cost, the ease of implementation in industry, and the wide quantity of lasers available, this technique is extremely important for machining glass.

Fabrication of microchannels on glass by laser ablation techniques has been investigated and reported using CO_2, UV, and ultrashort pulse lasers [16–19]. For transparent materials, in the visible spectral range, laser ablation should ideally be performed with ultraviolet radiation because of the linear optical absorption in this wavelength range. Alternatively, nonlinear coupling of ultrahigh-intensity laser pulses in the near-infrared (IR) range with subpicosecond

http://dx.doi.org/10.5772/64324

duration may show advantages. The interaction between a laser beam and a material is determined by (1) laser characteristics (the wavelength, fluence or energy density, the pulse duration, repetition rate, and pulse energy); (2) the properties of the material (absorption characteristics and thermal relaxation) which is governed by the composition and structure of the material.

In this context, laser micromachining, because of its noncontact nature, offers several advantages for fabricating microchannels, including the capability to form complex shapes with minimal mechanical and thermal deformation. There are still significant challenges in fabricating low-cost and reliable microfluidic modules in transparent media. In particular, microfluidic devices for detection of circulating tumor cells have emerged as a promising minimally invasive diagnostic tool. Isolation of circulating tumor cells (CTCs) has become a central topic in cancer research where engineering and medical science converge with the common goal of capturing rare cell types in liquid biopsies as a starting point for early diagnosis and the development of point of care and single-cell analysis systems [20]. Several designs have explored in Polydimethylsiloxane (PDMS) and glass substrates leading to panoply of features and arrangements able to trap cells flowing through the device. In order to enhance the specificity and sensibility of such systems, a surface functionalization with EpCAM antibodies seemed to be the first choice for developing a micropillar coating, such antibodies are commonly employed for CTC isolation.

Micropillars were some of the first features developed for studying cell behavior such as cell spreading, motility, and mechanobiology, but they present an interesting feature to be developed as a potential substrate prone to coating and exhibiting exceptional optical conditions for microscopy applications [21]. Therefore, functionalizing micropillars with a steady topographical control will be an optimal platform for a point-of-care device or lab-on-a-chip technology [22].

In this chapter, we present a laser-based technology for fabricating microfluidic microchannels and chips for circulating tumor cells capture. In particular, we report a fast and simple method for the fabrication of the microchannels on glass using an Nd:YVO_4 nanosecond IR laser. The fabrication method combines two different laser routes: (1) a laser direct-write technique for fabricating the microchannels on glass and (2) a thermal treatment for reducing the damage created on the glass during the laser direct-write process. By combining these two laser process, it is possible to obtain high-quality microchannels with comparable characteristics as those obtained by other methods [23], preserving the advantages of the laser direct-write technique (flexibility in terms of design, fast prototyping, low-cost, noncontaminant, etc). In Section 2, the experimental procedure for fabricating the microchannels is presented. Section 3 analyzes the thermal treatment and morphological characterization of microchannels as a function of temperature. Section 4 presents some conclusions and remarks.

2. Materials and methods

In order to perform the microstructuring of the glass a Rofin model Nd:YVO_4 laser was used. This is a solid-state laser, operating at 1064 nm wavelength and using a Q-Switch regime, with

pulses of 20 ns and tunable repetition rate from single-shot to 200 kHz. For the thermal treatment, we used a Heraeus mufla furnace, equipped with a thermal ramp that allows us to control the heating speed of the glass.

For characterizing the microstructures and samples, we have used a PerkinElmer Lamb25 spectrometer (for measuring the transmission spectrum); a scanning electron microscope (SEM, Zeiss FESEM-ULTRA Plus) for determination of the chemical composition, a microscope Nikon MM-400 (visual inspection of the samples), and a confocal microscope SENSOFAR 2300 Plμ (topographic and surface roughness measurement). Cell culture and trapping were assessed by means of a Zeiss Microscope and Zen software.

The glass used as a substrate for fabricating the microchannels and microstructures was a commercial soda-lime glass, provided by a local supplier. The composition of this glass (O 50.25%, Na 9.08%, Mg 2.19%, Al 0.54%, Si 33.08%, Ca 4.87%) was determined by using a SEM EDX (Zeiss FESEM-ULTRA Plus).

3. Results

3.1. Laser microstructuring

The laser direct-write technique for fabricating microfluidics devices and microchannels is based on the ablation of a soda-lime glass substrate with a beam laser of circular Gaussian profile, followed of a thermal treatment in a Heraeus mufla furnace. The laser setup for fabricating the micropost system consists of a Q-Switch Nd:YVO_4 laser operating at 1064 nm combined with a galvanometer system for addressing the output laser beam. The beam is focused by a flat-field lens of effective focal length 100 mm that provides a uniform irradiance distribution over a working area of 80 × 80 mm^2 (Figure 1). In order to perform the thermal treatment that allows us to improve the quality of the originally generated microchannels, a furnace Heraeus mufla was employed.

For optimizing the fabrication process, we have done a previous study of the mark obtained by focusing one laser shot on the glass substrate [24]. This mark was then analyzed with a confocal microscope. This initial characterization step let us to determine the optimal laser parameters used in the laser direct-write process. The microchannels morphology was analyzed in terms of shape and roughness using a confocal microscope SENSOFAR 2300 Plμ.

For determining the size of the mark made by the laser beam in the glass substrate, a crater was made in the glass after firing one shot at a fluence of 112 J/cm^2. The applied fluence was calculated by using the expression $F_{th} = (2E_{th})/(\pi\omega_0^2)$, where E_{th} is the energy per pulse at the onset of ablation, ω_0 was determined by analyzing the mark obtained by the laser over the material.

Because the measured Gaussian spot size on the surface is not necessarily equal to the calculated spot size at the focal point of the lens, the ablation threshold was computed using the following equation $\phi_{th} = (2E_{th})/(\pi\omega_0)$, where E_{th} is the laser energy at the ablation threshold

http://dx.doi.org/10.5772/64324

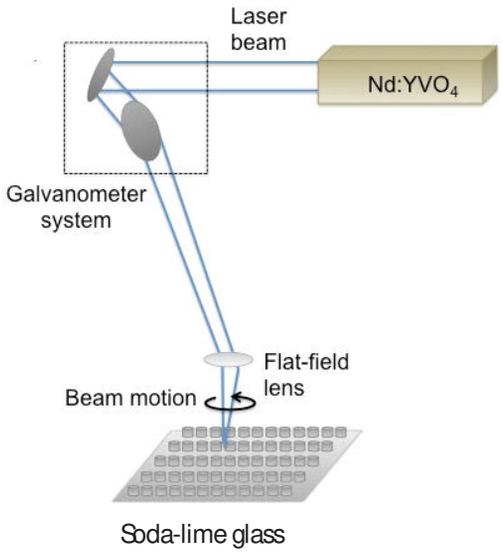

Figure 1. Laser setup for fabricating the microfluidic systems.

and ω_0 is the waist of the focal spot. Its value was obtained from the slope of the plot of $\ln(E_p/E_{th})$ against D^2 (diameter squared) ($D^2=2\omega_0^2 ln\left(\frac{E_p}{E_{th}}\right)$ see [25] for details) where E_p is the energy per pulse (Figure 2).

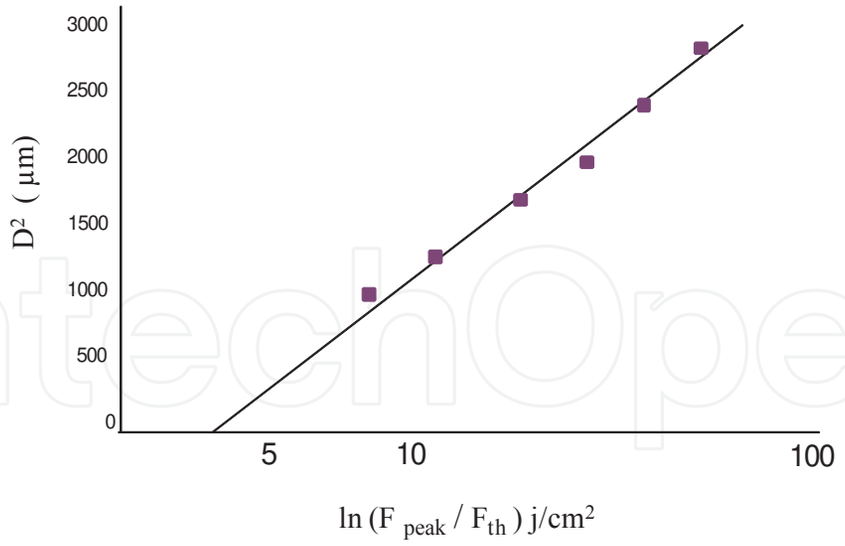

Figure 2. Linear relations between the squared diameter and the natural logarithm of the average laser fluences.

The main morphological parameters after laser ablation, such as depth and width for different number of pulses (fluence: 112 J/cm^2), have been analyzed using a confocal microscope SENSOFAR 2300 Plμ and an optical microscope Nikon MM-400.

Figures 3 and 4 show the evolution of the damage (diameter and depth) at the substrate surface with the number of pulses (1–10,000 pulses). Measurements of the depth and diameter of the ablated holes can also provide important information about the material response to the nanosecond laser.

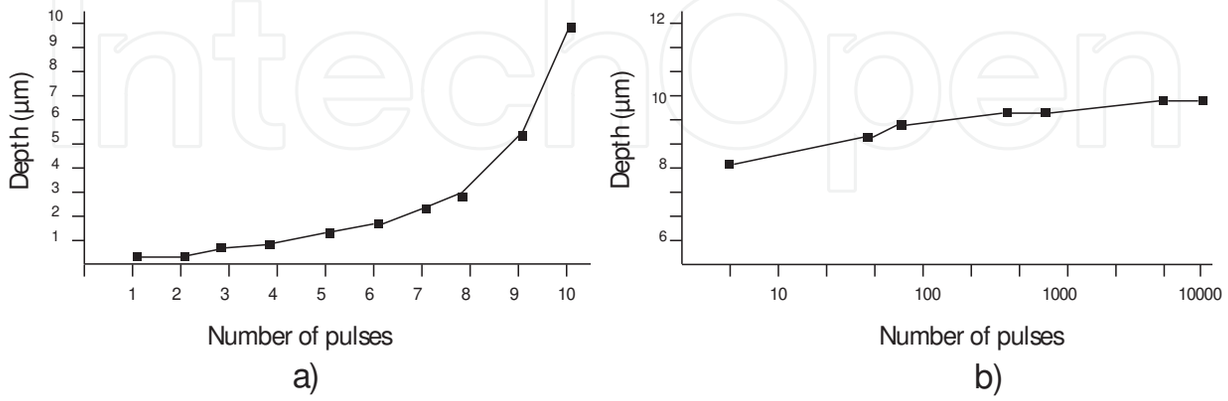

Figure 3. Evolution of depth versus number of pulses for (a) 1–10 pulses and (b) 10–10,000 pulses.

As shown in Figure 3a, the depth increases with the first pulses, reaching a depth value of 8 μm after 10 pulses, however after 10 pulses (Figure 3b), the depth increases slowly, varying only 2 μm after 500 pulses and maintain almost constant till 10,000 pulses. That behavior is due to the fact that the ablation plume does not have sufficient energy to take out the material detached on the ablation process.

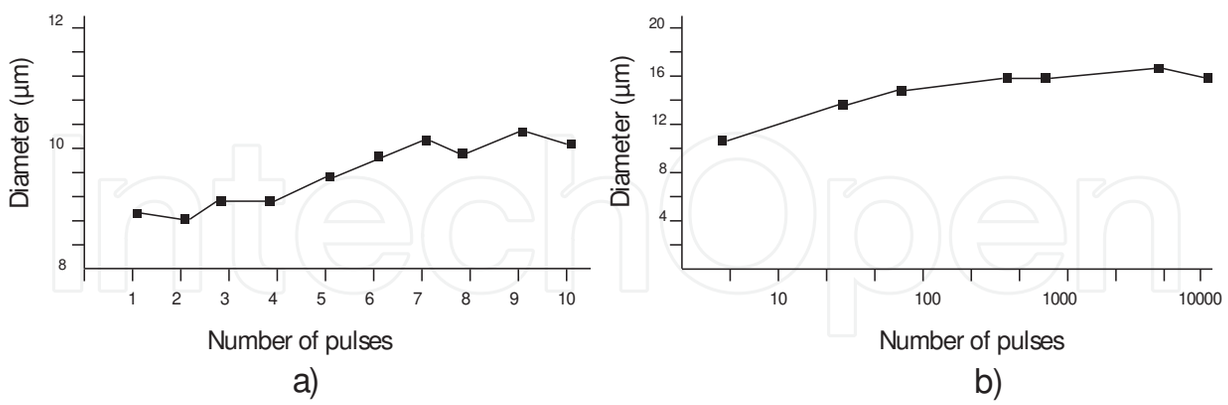

Figure 4. Evolution for diameter versus number of pulses: (a) 1–10 pulses and (b) 10–10,000 pulses.

From the slope obtained in Figure 4a, the evolution of diameter with the number of pulses can be deduced. The mark diameter increases slowly with the number of pulses, reaching a maximum value of depth 10 μm after 500 pulses, after this value (Figure 4b), increasing the number of pulses does not have a significant effect on the mark diameter.

http://dx.doi.org/10.5772/64324

For fabricating a homogeneous microchannel on glass, the optimization of the pulse overlaps, which determines the pulse per area is important to obtain quality microchannels. When the pulse overlap is high, there will be significant cracking in the microchannels edges because of the stress related with heat deposited in a small area. To obtain the optical pulse overlap, O_d, we use the following relation:

$$O_d = \left(1 - \frac{\upsilon}{2\omega_0 f}\right) \quad (1)$$

where υ is the galvoscanner speed, $2\omega_0$ is the focused spot diameter, and f is the laser repetition rate.

The first experimental approach for obtaining uniform channels was checked at different scan speeds for getting the optimal pulses overlapping (Figure 5). The same laser parameters (10 kHz, 8 W) were used for fabricating all the lines varying only the scan speed.

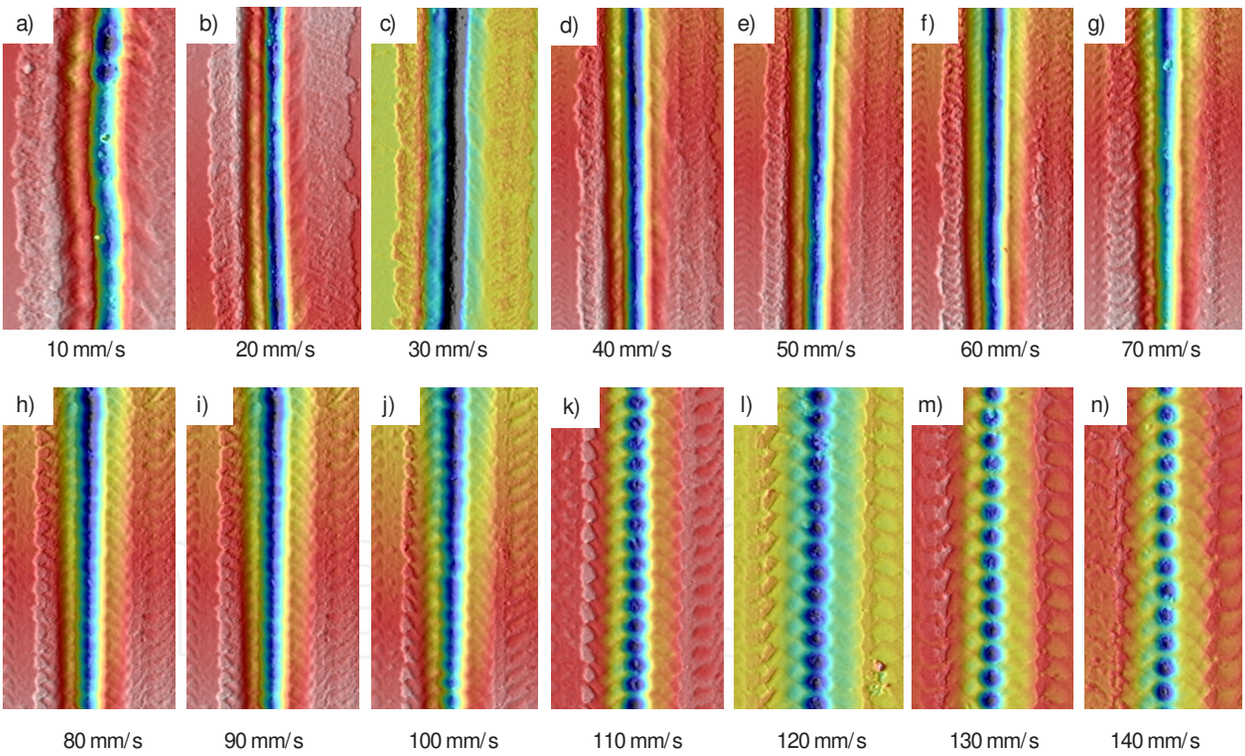

Figure 5. Confocal images of one microchannel obtained by laser ablation of glass at 10 kHz, 8 W for scan speeds values of (a) 10 mm/s, (b) 2 mm/s, (c) 30 mm/s, (d) 40 mm/s, (e) 50 mm/s, (f) 60 mm/s, (g) 70 mm/s, (h) 80 mm/s, (i) 90 mm/s, (j) 100 mm/s, (k) 110 mm/s, (l) 120 mm/s, (m) 130 mm/s, and (n) 140 mm/s.

As it can be appreciate in Figure 5, the best results were obtained for the channels fabricated between 40 and 80 mm/s (Figure 5d and h). At low scan speed, the high overlapping of the pulses delivers too much energy at the surface, which leads to an irregular channel. Low

overlapping creates a distortion on the microchannels (Figure 5j–n). For scan speeds higher than 80 mm/s, it can be appreciated the interaction of one pulse with the substrates (Figure 5a–c), which also increase the roughness average and does not allow the formation of the microchannels. Figure 6 shows the pulse overlap, obtained using Eq. (1), and the roughness average measured at different scan speeds. In terms of pulse overlap (Figure 6a), values in the range of 60–80% are needed for fabricating microchannels with good qualities. For scan speed values in the interval of 40–80 mm/s, roughness around 55 nm is obtained (Figure 6b).

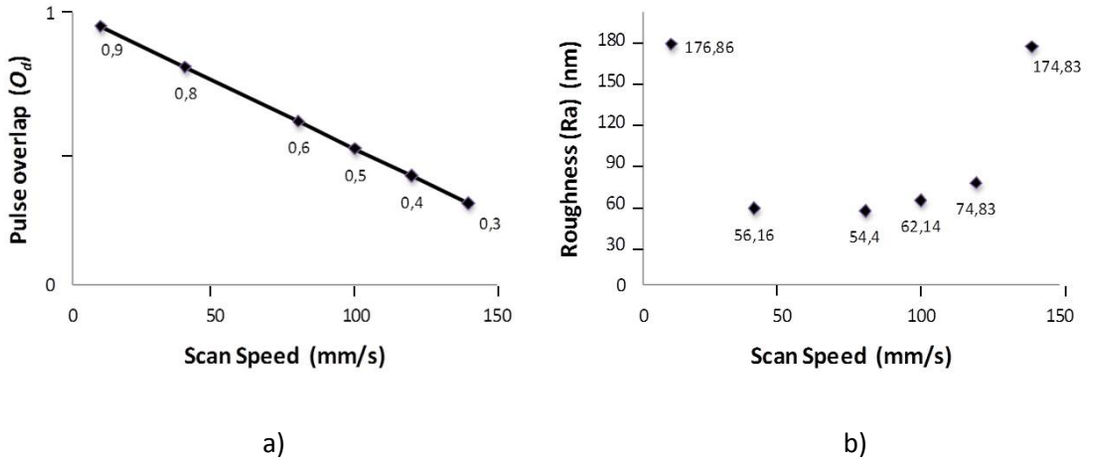

Figure 6. (a) Evolution of pulse overlap and (b) roughness versus scan speed in the range of 10–140 mm/s.

Figure 7 shows a microchannel fabricated using the optimal pulse overlap obtained from the study presented above, and laser parameters of 8 W, 10 kHz and scan speed of 50 mm/s. The resulting channel exhibits a surface roughness of 54 nm with a diameter of 8 μm and height of 3 μm.

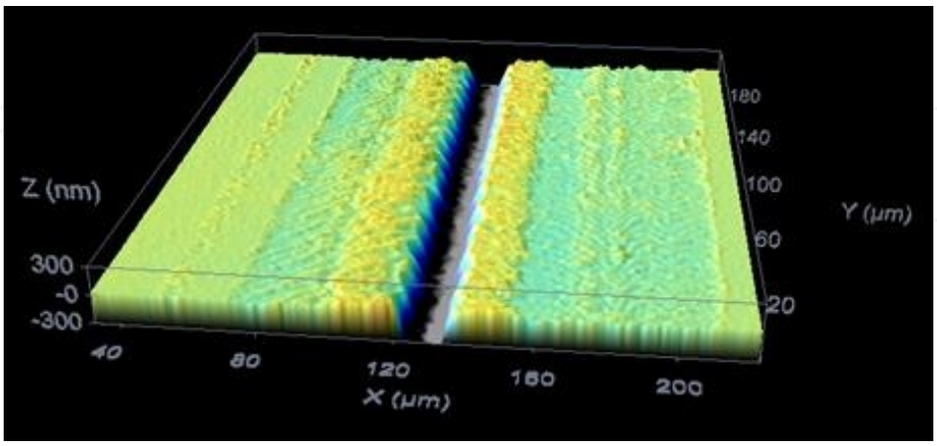

Figure 7. Initial microchannel fabricated by laser ablation.

In order to fabricate different microchannels configurations, a study of the evolution of depth and diameter with the number of laser passes over the same place was done (laser parameters:

http://dx.doi.org/10.5772/64324

8 W, 10 kHz and scan speed 50: mm/s). Figure 8 shows the evolution of depth and diameters varying the number of laser passes.

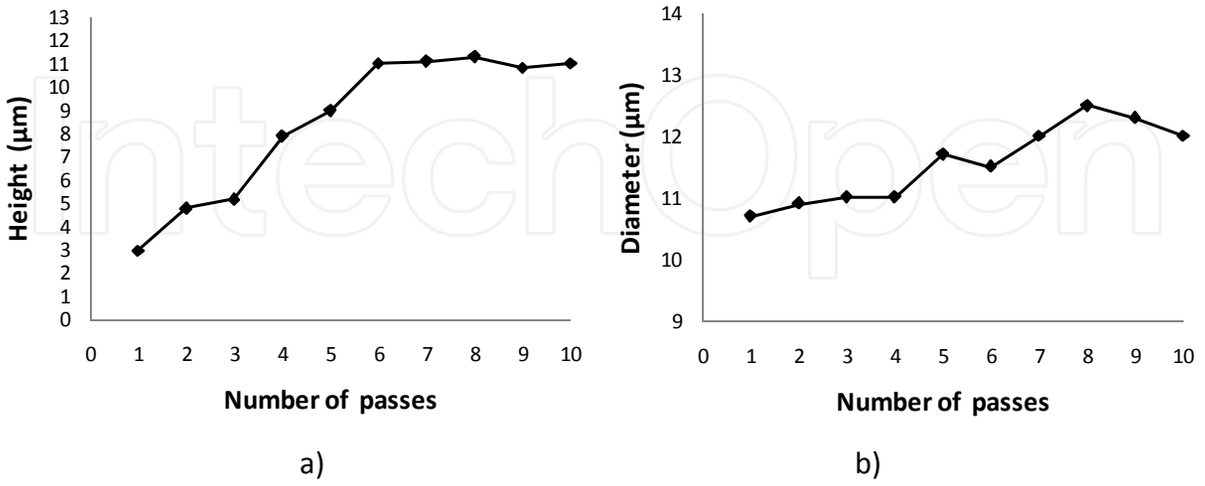

Figure 8. (a) Evolution of depth and (b) diameter with the number of laser passes.

It is evident from Figure 8 that the channel aspect ratio $\alpha = h/d$ varies with the number of passes. The diameter d reaches its saturation value after five laser passes, increasing just around 200 nm per laser pass and varying only 1 μm after five passes, above these values the diameter is maintained almost constant. In contrast, the ablation height h changes dramatically with the increase in number of pulses, after 6 passes this value remains constant. The height increases 1 μm per laser pass, up to a value of 12 μm. We can relate this behavior with the nonevacuation of the debris generated during laser ablation process that arise from the bottom of the microchannels and also because to the lack of focus as the depth of the microchannel increases. The diameter of the microchannel is maintained almost constant by increasing the number of laser passes, which can be related with the diameter of the laser beam used.

One of the important challenges to overcome using a laser direct-write process for fabricating microchannels in glass is to obtain good-quality junctions. The propelled material of the subsequent channels is deposited on the existing microchannel that turns into a bad quality of the microchannel. This debris changes the average roughness, and because it is crucial for obtaining high-quality elements, the microchannels were cleaned after laser exposure using chemical etching process of hydrofluoric acid (HF). The HF acid is an etchant that attacks glasses at significant high-etch rate [16]. Commercial soda-lime glass used in this work is composed of SiO_2 (73.8%), Na_2O (12.7%), CaO (8.6%), MgO (4.1%), Fe_2O_3 (0.14%), and Al_2O_3 (0.1%). Etching soda-lime glass in an HF solution forms insoluble products that are believed to be mainly CaF_2 and MgF_2.

The etching time, concentration of the acid, and the temperature of the process are important parameters to control the HF cleaning process. In terms of handle, HF is a strong corrosive and highly toxic at higher concentrations. The etching process was performed at 10% HF concentration, which in terms of security reduces considerably percentages of toxic vapor that

contaminates the work space. Figure 9 shows a SEM top view image of one microchannel before (Figure 9a) and after (Figure 9b) HF etching.

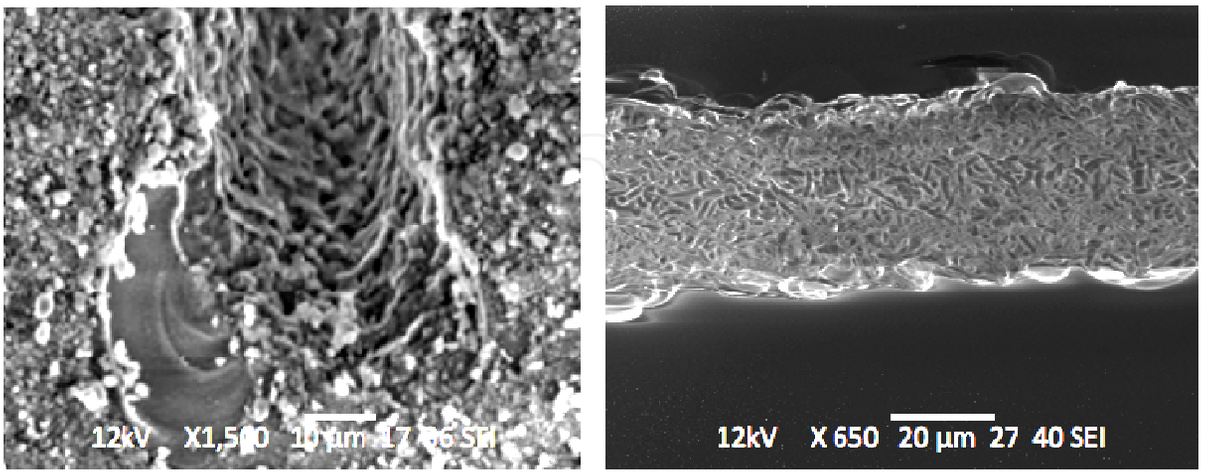

a) b)

Figure 9. SEM image of the microchannel top surface (a) before chemical etching and (b) after 10 min in 10% HF aqueous solution.

In Figure 9a, debris deposited on the top of the microchannels during the laser ablation can be observed. In Figure 9b, after chemical etching, the debris was successfully eliminated.

3.2. Thermal treatment

A thermal treatment was applied into an oven to obtain the final elements and to improve the morphological properties. The samples were reflown in a Heraeus mufla furnace for 2 h at temperatures between 620°C and 670°C (steps of 10°C). The working range has been chosen to be higher than the glass transition temperature of soda-lime glass (T_g =564°C). Figure 10 shows a 3D confocal image of microfluidic microchannels fabricated at different reflow temperatures.

As shown in Figure 10, at 620°C, there was not a significant modification in the surface shape, and at temperatures higher than 670°C, the initial shape surface profile becomes flat so that microchannels obtained by laser direct-write disappear.

This displacement of material due to the thermal treatment and the accumulation in the bottom turns into a reduction in height while the diameter is increased due to the material reflow from the top of the edges of the microchannels at the bottom of the crater. This effect allows both the thermal reflow and to fill the irregular structure of crater with material leading to an improvement on the morphological qualities.

The flow resistance for each microchannel depends on the geometry and roughness. The surface roughness on the wall of the microchannel increases when the flow rate decreases, so

http://dx.doi.org/10.5772/64324

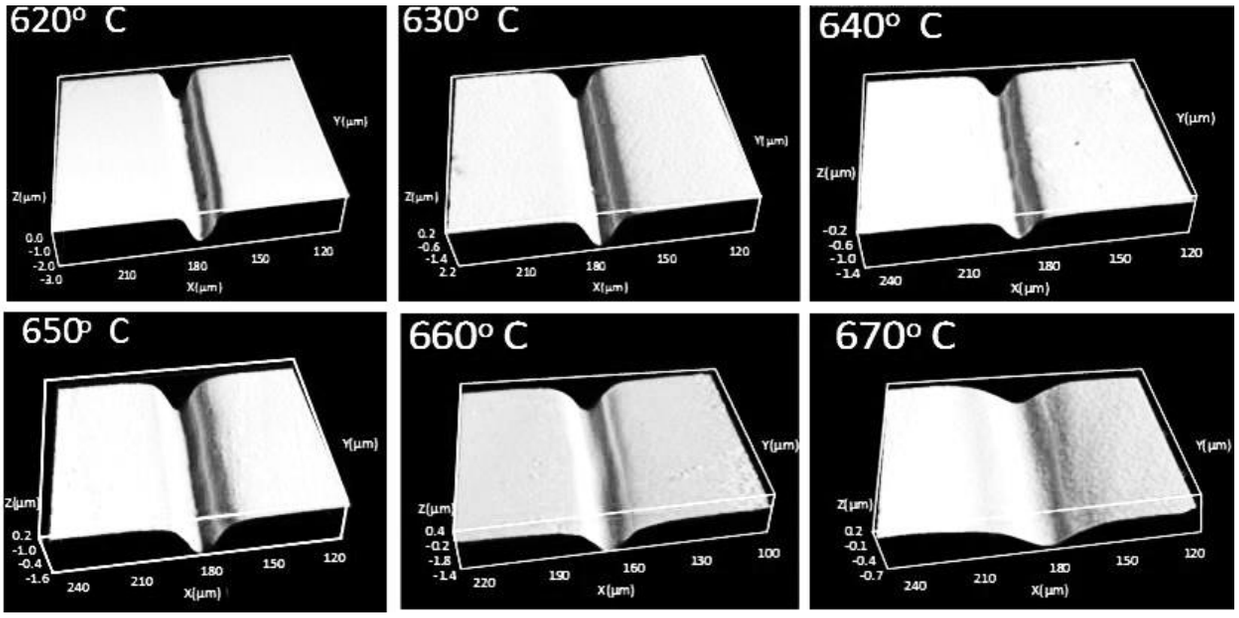

Figure 10. Confocal images of microchannels obtained after thermal treatment at different temperatures. Six different results at different reflow temperatures are shown: T_1 = 620°C, T_2 = 630°C, T_3 = 640°C, $T4$ = 650°C, $T5$ = 660°C, and $T6$ = 670°C.

the change of hydraulic resistance is proportional to the change in the surface roughness. For determining the quality of the microchannels fabricated at different thermal reflow temperatures, it was determined the roughness at the bottom of the channels [26]. Table 1 shows the evolution of roughness for temperatures between 620 and 670°C, taken at steps of 10°C. The purpose of thermal treatment is to reduce the roughness generated during the laser direct-write process. It is important to find a compromise between shape modification and roughness. The shape should be maintained whereas the thermal reflow should reduce the surface roughness.

Temperature (°C)	Ra (nm)
Ra glass surface	3.68
Ra after laser ablation	640
620	125.14
630	57.14
640	39.45
650	29.40
660	16.43
670	7.35

Table 1. Comparative of roughness evolution with thermal reflow.

In order to study the microfluidics capabilities of our technique, after obtaining the best parameters for fabricating optimal microchannels, we focused on fabricating microchannels with different configurations trying to solve the main problems related with the laser ablation of glass, in particular for creating uniform and debris-free channels. Figure 11 shows some microchannels fabricated using the laser direct-write technique.

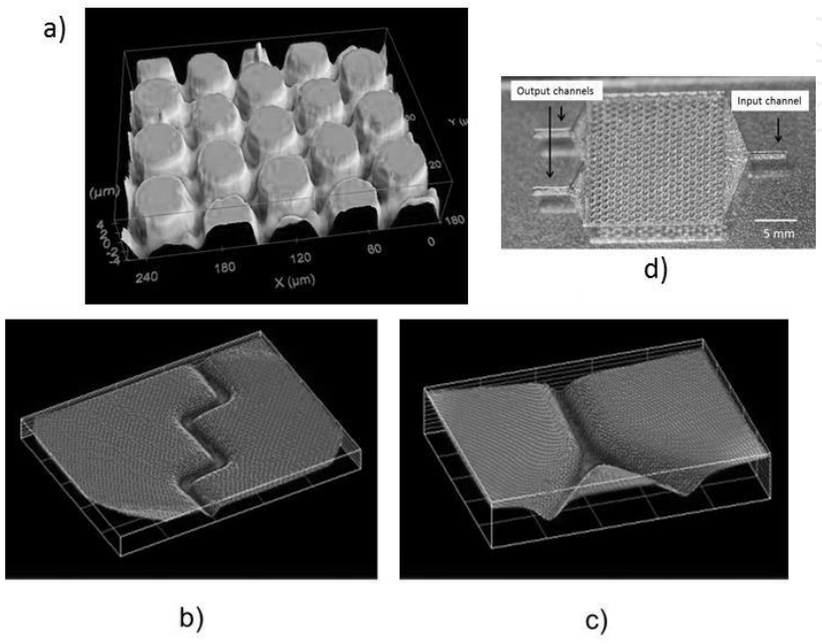

Figure 11. Microfluidics microchannels fabricated using the laser direct-write technique.

3.3. Biochip for capturing circulating tumor cells

In the previous work, we have demonstrated the suitability of the presented technique for fabricating a circulating tumor cell biochip [20]. The biochip is composed of a group of micropost (see Figure 11a), integrated in a microfluidics devices (see Figure 11d) for capturing circulating tumor cells. Using the aforementioned laser technique, we have fabricated an input channel for perfusing the media and two outputs channels for media removal (Figure 11d). The microfluidics devices were covered with a microscope cover slide (100 μm thickness). The manufactured chips were tested for detection of tumor cells (Hec 1A) after being functionalized with an EpCAM antibody coating. Cells were flown with media through the device allowing an interaction with the functionalized micropillars. After eluting the whole sample, chips were assessed for sensitivity and efficiency under a confocal microscope.

Fluorescently stained (DiO) CTCs were counted the cell trapping array region of the biochip using epifluorescent microscope (Zeiss Axio Vert A.1) was equipped with a 20× objective (Zeiss, numerical aperture = 0.4) and a low-light CCD camera.

Figure 12 shows the resulting cell isolation from cells flown in media. Pillars were able to trap circulating cells pumped in the device.

http://dx.doi.org/10.5772/64324

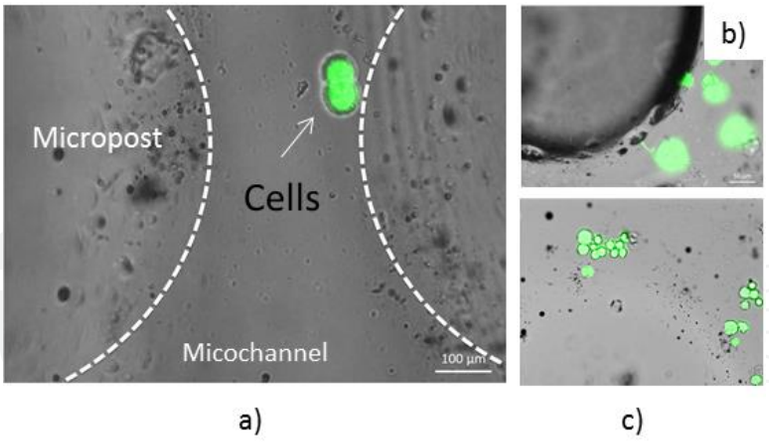

Figure 12. Cells attachment to the functionalized surface is observed in (a), (b), or (c). Cells are strongly bonded to the antibody surface and are not detached under flow conditions (white arrows show the location of the cells).

Pictures were taken along the device, there is a heterogeneous distribution for cell isolation along the posts while due to the chip dimensions few cells were found on the bottom (Figure 12c). In accordance to the surface functionalization protocol, the whole chip was coated with EpCAM antibodies, hence the bottom areas should be able to detain cells as well.

4. Conclusions

A hybrid method for fabricating microfluidic microchannels and a biochip for CTCs on soda-lime glass has been developed. The fabrication process consists of a combination of the laser direct-write technique for promoting glass structures and a thermal treatment for reshaping and or improving the morphological qualities of the generated microchannels. By applying the thermal treatment at 620°C (during 2 h), we are able to obtain high-quality microchannels maintaining the initial shape. This treatment allows us to reshape and improve the morphological, in terms of roughness, and optical qualities, in terms of transparency, of the generated microfluidics structures. This approach is a rapid and low-cost procedure to obtain glass microstructures where a chemical modification can take place, leading to the possibility of performing surface modifications with EpCAM antibodies to successfully stop circulating tumor cells. Therefore, the presented glass platform in this chapter can provide a good starting point to develop more complex systems aimed for single-cell analysis and isolation leading to a primary culture.

Acknowledgements

This work was supported by Xunta de Galicia, Spain, under Galician Programme for Research Innovation and Growth 2011–2015 (I2C Plan). We would also like to thank to Ramiro Couceiro for his assistance with the biological trials and confocal images.

Author details

Daniel Nieto García[1,2*] and Gerard O'Connor[2]

*Address all correspondence to: daniel.nieto@usc.es

1 Microoptics and GRIN Optics Group, Applied Physics Department, Faculty of Physics, University of Santiago de Compostela, Santiago de Compostela, Spain

2 School of Physics, National Centre for Laser Applications, National University of Ireland, University Road, Galway, Ireland

References

[1] D. Erickson and D. Li. Integrated microfluidic devices. Analytica Chimica Acta. 2004;507:11–26.

[2] Y. Cheng, K. Sugioka and K. Midorikawa. Microfluidic laser embedded in glass by three-dimensional femtosecond laser microprocessing. Optics Letters. 2004;29(17): 2007–2009.

[3] F. Cattaneo, K. Baldwin, S. Yang, T. Krupenkine, S. Ramachandran and J.A. Rogers. Digitally tunable microfluidic optical fiber devices. Journal of Microelectromechanical Systems, 2003;12(6):907–912.

[4] G.M. Whitesides. The origins and the future of microfluidics. Nature. 2006;442:368–373.

[5] T. Rajabi, V. Huck, R. Ahrens, M.C. Apfel, S.E. Kim, S.W. Schneider and A.E. Guber. Development of a novel two-channel microfluidic system for biomedical applications in cancer research. Biomedical Engineering. 2012; 57:921–922.

[6] C.W. Huang and G.B. Lee. A microfluidic system for automatic cell culture. Journal of Micromechanics and Microengineering. 2007; 17(7):1266.

[7] H. Andersson, A. Van Den Berg. Microfabrication and microfluidics for tissue engineering: state of the art and future opportunities. Lab Chip. 2004;4:98–103.

[8] M.S. Giridhar, K. Seong, A. Schülzgen, P. Khulbe, N. Peyghambarian, and M. Mansuripur. Femtosecond pulsed laser micromachining of glass substrates with application to microfluidic devices", Applied Optics. 2004: 43(23):4584–4589.

[9] Y. Li, S. Qu and Z. Guo. Fabrication of microfluidic devices in silica glass by water-assisted ablation with femtosecond laser pulses. Journal of Micromechanics and Microengineering. 2011;21:075008.

[10] J.Y. Cheng, M.H. Yen, C.W. Wei, Y.C. Chuang and T.H. Young. Crack-free direct-writing on glass using a low-power UV laser in the manufacture of a microfluidic chip Journal of Micromechanics Microengineering. 2005; 15:1147–1156.

[11] H. Becker and U. Heim. Hot embossing as a method for the fabrication of polymer high aspect ratio structures. Sensors and Actuators. 2000; 83:130–135.

[12] D. Martin Knotter. Etching mechanism of vitreous silicon dioxide in HF-based solutions. Journal of American Chemical Society, 2000;122(18):4345–4351.

[13] P.A. Clerc, L. Dellmann, F. Gretillat, M.A. Gretillat, P.F. Inderm, S. Jeanneret, Ph. Luginbuhl, C. Marxer, T.L. Pfeffer, G.A. Racine, S. Roth, U. Staufer, C Stebler, P. Thiebaud and N.F. de Rooij. Advanced deep reactive ion etching: a versatile tool for microelectromechanical systems. Journal of Micromechanics and Microengineering. 1998;8:272–278.

[14] G. Kopitkovas, T. Lippert, J. Venturini, C. David and A. Wokaun. Laser induced backside wet etching: mechanisms and fabrication of micro-optical elements. Journal of Physics: Conference Series. 2007;59:526–553.

[15] M. Wakaki, Y. Komachi, and G. Kanai. Microlenses and microlens arrays formed on a glass plate by use of a CO_2 laser. Applied Optics. 1998; 37:627–631.

[16] I.K. Sohn, M.S. Lee, J.S. Woo, S.M. Lee and J.Y. Chung. Fabrication of photonic devices directly written within glass using a femtosecond laser. Optics Express. 2005;13(11):4224–4229.

[17] M.T. Flores-Arias a, A. Castelo, C. Gomez-Reino and G.F. de la Fuente. Phase diffractive optical gratings on glass substrates by laser ablation. Optics Communications 2009; 282:1175–1178.

[18] M. Stjernström and J. Roeraade. Method for fabrication of microfluidic systems in glass. Journal of Micromechanics and Microengineering. 1998; 8:33.

[19] D. Nieto, M.T. Flores-Arias, G. O'Connor and C. Gomez-Reino. A Laser direct-write technique for fabricating microlens arrays on soda lime glass with a Nd:YVO_4 laser. Applied Optics. 2010; 49(26):4979–4983.

[20] S.L. Stott, C.H. Chia-Hsien Hsu, D.I. Tsukrov, M. Yu and D.T. Miyamoto. Isolation of circulating tumor cells using a microvortex-generating herringbone-chip. Proceedings of the National Academy of Sciences of the United States of America. 2010;107:18392–18397.

[21] Y. Dong, A.M. Skelley, K.D. Merdek, K.M. Sprott, C. Jiang. Microfluidics and circulating tumor cells. The Journal of Molecular Diagnostics. 2013;15:149–157.

[22] B. Cheng, H. Song, S. Wang, C. Zhang, B. Wu, Y. Chen, F. Chen and B. Xiong. Quantification of rare cancer cells in patients with gastrointestinal cancer by nanostructured substrate. Translational Oncology. 2014;7(6):720–725.

[23] D. Nieto, R. Couceiro, M. Aymerich, R. Lopez-Lopez, M. Abal and M.T. Flores-Arias. A laser-based technology for fabricating a soda-lime glass based microfluidic device for circulating tumour cell capture. Colloids and Surfaces B: Biointerfaces, 2015;134:363–369.

[24] D. Nieto, M.T. Flores-Arias, G. O'Connor and C. Gomez-Reino. A Laser direct-write technique for fabricating microlens arrays on soda lime glass with a Nd:YVO_4 laser. Applied Optics. 2010;49(26):4979–4983.

[25] A. Ben-Yakar and Robert L. Byer, Femtosecond laser ablation properties of borosilicate glass. Journal of Applied Physics. 2004;96:5316–5323.

[26] D. Nieto, T. Delgado and M.T. Flores-Arias. Fabrication of microchannels on soda-lime glass substrates with a Nd:YVO_4 laser. Optics and Lasers in Engineering. 2014;63:11–18.